1. AGENCY USE ONLY (Leave blank)	2. REPORT DATE	3. REPORT TYPE AND DATES COVERED
	02/17/93	Final Tech.Report 12/01/89 - 01/31/93

4. TITLE AND SUBTITLE

Studies of Origin of Three-Dimensionality in Laminar Wakes

5. FUNDING NUMBERS

N00014-90J-1314

6. AUTHOR(S)

Morteza Gharib/Principal Investigator

7. PERFORMING ORGANIZATION NAME(S) AND ADDRESS(ES)

The Regents of the University of California
University of California, San Diego
Office of Contracts & Grants Admin, 0934
9500 Gilman Drive
La Jolla, Ca. 92093-0234

8. PERFORMING ORGANIZATION REPORT NUMBER

9. SPONSORING/MONITORING AGENCY NAME(S) AND ADDRESS(ES)

Office of Naval Research
Ocean Engineering, Code 11210T
800 North Quincy St.
Arlington, VA 22217-5000
Attn: Mr. Steven Ranberg, Mechanics, Rm. 663

10. SPONSORING/MONITORING AGENCY REPORT NUMBER

11. SUPPLEMENTARY NOTES

Submitted to the Journal of Fluid Mechanics, November, 1992.

12a. DISTRIBUTION/AVAILABILITY STATEMENT

DISTRIBUTION STATEMENT

Approved for public release;
Distribution Unlimited

423 238

13. ABSTRACT (Maximum 200 words)

Wind tunnel experiments, using hot-wire anemometry and smoke-wire flow visualization, were conducted to study the process of transition from laminar to turbulent flow of parallel and oblique vortex streets from circular cylinders. It was found that the origin and scale of three-dimensionality which appears at Reynolds numbers just below the transition from laminar to turbulent flow are dependent on the vortex shedding geometry in the near-wake. Oblique vortex streets develop large scale three-dimensional structures and undergo an early transition, i.e. at lower Reynolds numbers, when compared to parallel vortex streets. This is due to the presence of three-dimensionality in oblique wakes at pre-transition Reynolds numbers, whereas parallel wakes remain laminar until the vortices themselves develop three-dimensional features.

The downstream evolution of these two wake geometries from the primary Kármán vortices to the far-wake vortical structures was also investigated. The far-wake structures are parallel to the cylinder axis for parallel shedding. For oblique shedding, these structures are initially parallel to the cylinder axis, but further downstream they develop a strong spanwise modulation whose wavelength is the spanwise distance between two consecutive Kármán vortices of the same sign of vorticity.

14. SUBJECT TERMS			15. NUMBER OF PAGES 30
			16. PRICE CODE
17. SECURITY CLASSIFICATION OF REPORT	18. SECURITY CLASSIFICATION OF THIS PAGE	19. SECURITY CLASSIFICATION OF ABSTRACT	20. LIMITATION OF ABSTRACT

Evolution of three-dimensionality in the wake of a circular cylinder at low Reynolds numbers

M. Hammache and M. Gharib

Department of Applied Mechanics and Engineering Sciences
University of California, San Diego
La Jolla, CA 92093-0402

Abstract:

Wind tunnel experiments, using hot-wire anemometry and smoke-wire flow visualization, were conducted to study the process of transition from laminar to turbulent flow of parallel and oblique vortex streets from circular cylinders. It was found that the origin and scale of three-dimensionality which appears at Reynolds numbers just below the transition from laminar to turbulent flow are dependent on the vortex shedding geometry. Oblique vortex streets develop large scale three-dimensional structures and undergo the transition to turbulence prematurely, i.e. at lower Reynolds numbers, when compared to parallel vortex streets.

The downstream evolution of these two wake geometries from the primary Kármán vortices to the secondary vortices of the far-wake was also investigated. The far-wake vortex structures are parallel to the axis of the cylinder in the case of parallel shedding. For oblique shedding, the far-wake structures are also initially parallel to the axis of the cylinder but further downstream they become strongly modulated in the spanwise direction. The wavelength of this modulation is equal to the spanwise wavelength in the near-wake, i.e. the spanwise distance between two consecutive Kármán vortices of the same sign of vorticity.

Introduction:

The three-dimensional transition to turbulence of bluff body wakes has been the object of considerable attention in the last few decades. In particular, an understanding of the scenario of first appearance of three-dimensionality and its contribution to the transition process has been an important part of the study of circular cylinder wakes.

In a recent surge of interest in parallel and oblique vortex shedding from circular cylinders, a number of techniques have been developed to induce parallel vortex shedding, e.g. Williamson (1988), Hammache and Gharib (1989), Eisenlohr and Eckelmann (1989). Subsequently, Hammache and Gharib (1991) conducted wind and water tunnel experiments primarily aimed at understanding the mechanism responsible for the oblique vortex shedding from circular cylinders, and determined conclusively that this phenomenon is due to a base pressure imbalance between the cylinder ends. This pressure imbalance in turn induces a mean spanwise flow in the back stagnation region of the cylinder. This spanwise flow was found to persist in the wake itself, i.e. several diameters downstream of the cylinder, where it is thought to be a result of induction by the oblique vortices.

The motivation for the present work was sparked by two important observations on the behavior of oblique vortex streets:

1. In Hammache and Gharib (1989) we reported that the parallel and oblique wakes undergo the three-dimensional transition to turbulence at different values of the Reynolds number. In the case of the oblique shedding, as the flow velocity is increased, a transition occurs in the nature and uniformity of the vortex filaments in the near field, which leads to the transition to turbulent flow. In contrast, when the parallel shedding is maintained, the vortex street remains laminar and parallel and the transition is delayed up to a higher value of the Reynolds number. It was thus concluded that the oblique vortex street undergoes the laminar-turbulent transition prematurely, or, conversely, that inducing parallel shedding inhibits the development of three-dimensionality in the wake.

2. By towing circular cylinders and flat plates in water tanks, Taneda (1959) observed that the original Kármán vortex street breaks down at some distance downstream of the cylinder and that new vortical structures of larger scale and lower frequency emerge to form what he called a "secondary vortex street". This structure also decays further downstream and another cycle of wake re-arrangement starts, and so on. He suggested that the process of growth and decay of vortical structures at various frequencies is governed by hydrodynamic instability. Cimbala, Nagib and Roshko (1988) conducted wind tunnel experiments on circular cylinder wakes and also observed the decay of the primary vortex street and the emergence and growth of a secondary vortex structure. Their hot-wire measurements showed conclusively that hydrodynamic instability was indeed the mechanism for the wake rearrangement. In one of their smoke-wire flow visualizations (their Figure 19), one can see that the primary Kármán vortex street was oblique and that the secondary vortices were strongly modulated in the spanwise direction. This has also been observed by Williamson (1992) at the 1992 IUTAM symposium on bluff body wakes, dynamics and instabilities.

No previous attempt has been made to investigate possible links between the two aspects of oblique vortex shedding described above. Our objective is to examine the effect of the vortex shedding condition (i.e. parallel or oblique) on the evolution of the wake:

1. with the Reynolds number, at a given location behind the cylinder in the near-wake.

2. with the downstream distance, at a given value of the Reynolds number (below transition).

These two aspects of the study would provide important information on the scales of three-dimensionality present in the wake prior to the transition to turbulence and how these scales influence the downstream evolution of the wake, past the region of decay of the Kármán vortices. Note that the term "near-wake" used throughout this paper denotes the original Kármán vortex street, and not just the immediate vicinity of the cylinder. Simple experiments, which rely on flow visualization and hot-wire measurements and which take advantage of our technique to control the angle of shedding, are conducted in order to compare the scenarios of transition to turbulence of parallel and oblique wakes and their downstream development into the far-wake.

Experimental setup:

All experiments were conducted in a low-speed, low-turbulence, recirculating wind tunnel with a square test section of 20.96 cm by 20.96 cm. Figure 1 illustrates the setup and coordinate system.

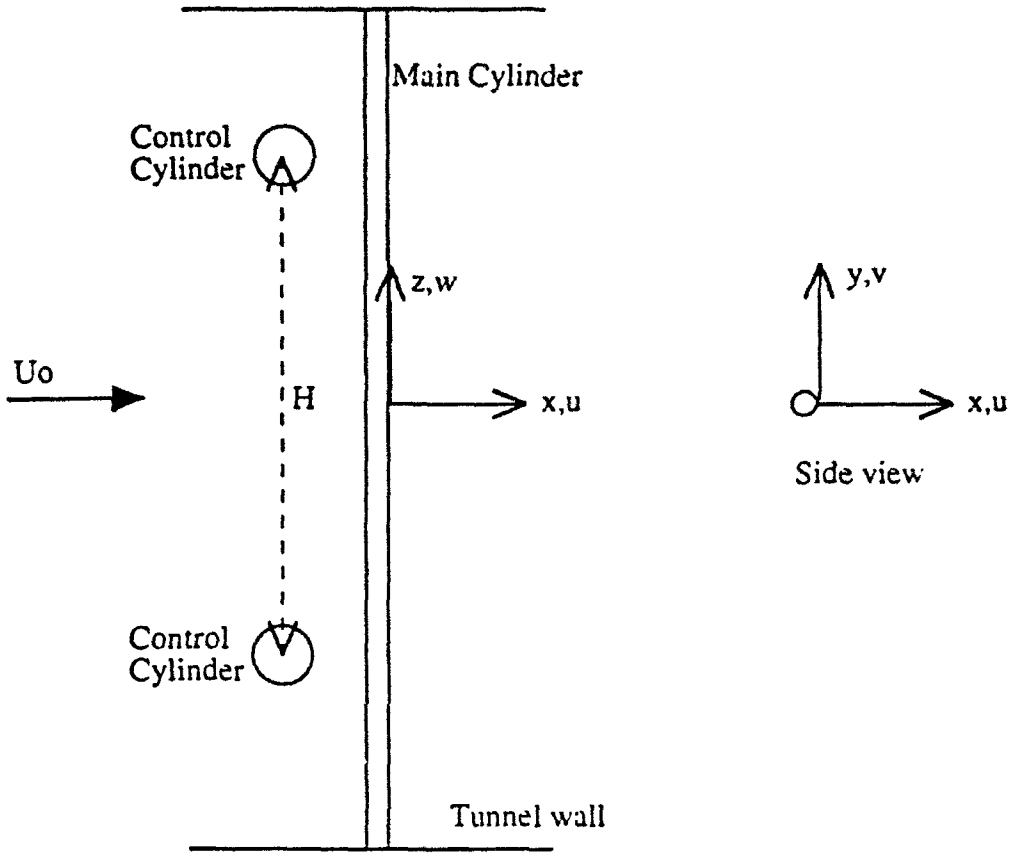

Figure 1. Experimental setup and coordinate system

The main cylinder was a stainless steel hypodermic tube of high diameter consistency and very smooth surface finish, and the control cylinders were stainless steel drill rods. The plan view of the wake was visualized by using the smoke-wire technique with the ability to position the smoke-wire at various locations downstream of the cylinder and at one edge of the Kármán vortex street, so that only one side of the vortex street is traced. For a detailed description of the technique used to control the vortex shedding, the reader is referred to Hammache and Gharib (1991).

The velocity measurements were taken with a hot-wire mounted on a three-axis traversing mechanism. In some instances, we added a second hot wire which could be moved with respect to the first one in the spanwise direction. Using two hot-wires allowed us to measure the spanwise

wavelength in the near-wake, i.e. the spanwise distance between two consecutive vortices of the same sign. The coordinate system is such that x, y and z are in the streamwise, cross-stream and spanwise directions respectively, with the origin at the back stagnation point and mid-span of the cylinder.

Evolution of parallel and oblique near-wakes with the Reynolds number:

Hot-wire velocity measurements were obtained for the parallel and oblique vortex shedding in the Reynolds number range 135-170, at 12 diameters downstream of the cylinder. Fast-Fourier transforms were performed on the velocity data and smoke-wire flow visualization photographs were taken.

The parallel shedding was obtained with the control cylinder technique. As the Reynolds number is gradually increased, the wake which was kept parallel all along became turbulent at Re≈164. This sharp transition is illustrated in Figures 2 and 3 taken at Re≈162 and ≈164 respectively. The averaged hot-wire spectra corresponding to these two flow regimes are shown in Figures 4 and 5 respectively. While the spectrum in Figure 4 is dominated by a sharp peek at the shedding frequency, the one in Figure 5 is broad-band, with a higher low-frequency turbulence level. Note that the values of the Reynolds number mentioned above may vary with the effective aspect ratio (H/d) of the cylinder. Nonetheless, the qualitative behavior remains the same regardless of the cylinder aspect ratio: the initially parallel wake undergoes a sharp transition from laminar to turbulent.

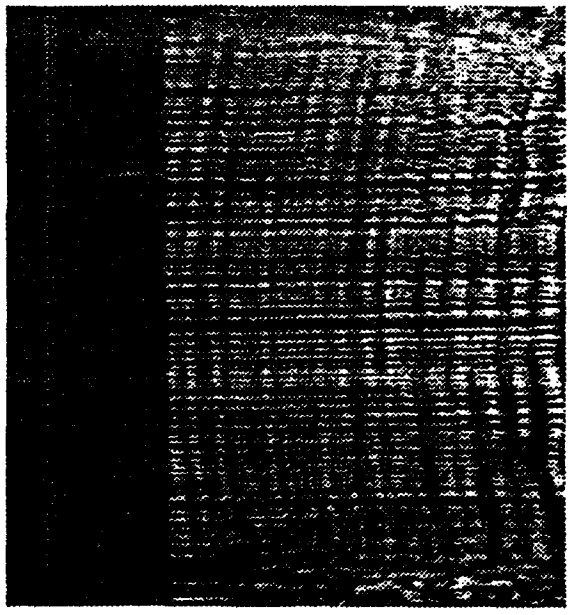

Figure 2. Flow visualization of laminar parallel shedding at Re=162. d=0.157cm, H/d=160. Smoke-wire at x/d=25.

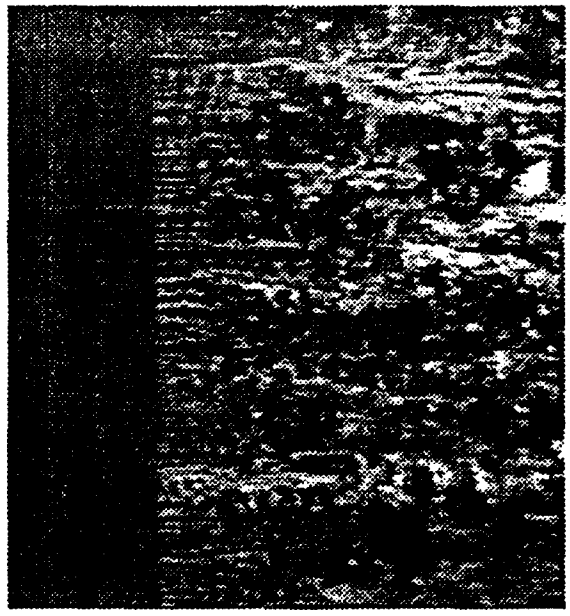

Figure 3. Flow visualization of turbulent shedding at Re=164. d=0.157cm, H/d=160. Smoke-wire at x/d=25.

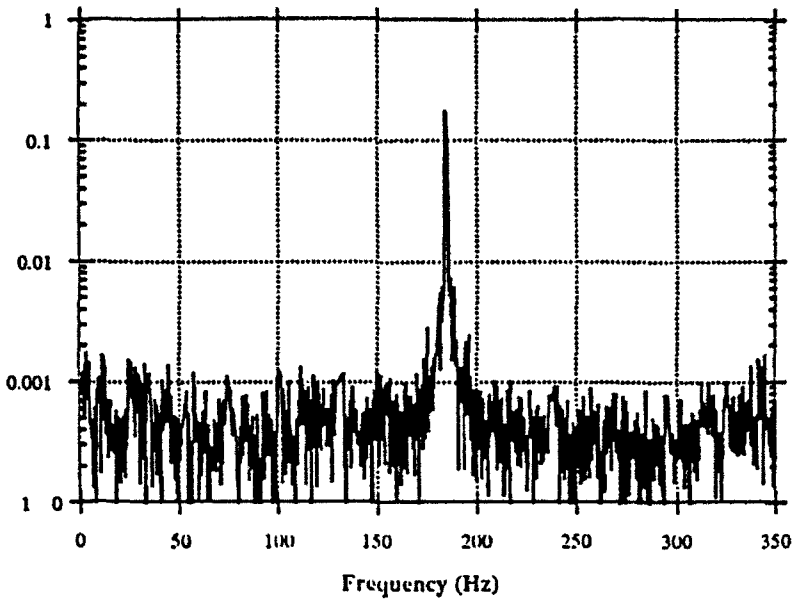

Figure 4. Time-averaged velocity spectrum of laminar parallel shedding at Re=162. d=0.157cm, H/d=160. Hot-wire at x/d=12.

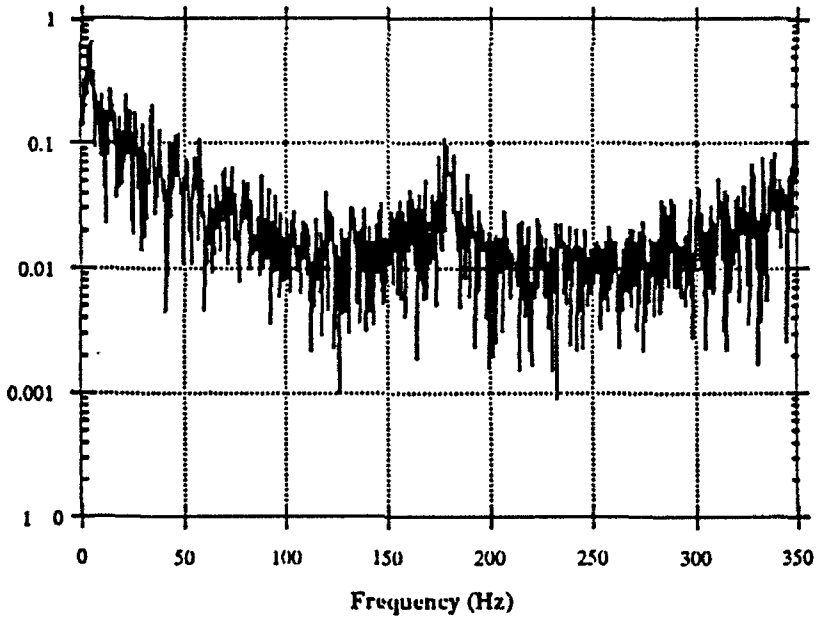

Figure 5. Time-averaged velocity spectrum of turbulent shedding at Re=164. d=0.157cm, H/d=160. Hot-wire at x/d=12.

The behavior of the oblique wake as the Reynolds number is increased turned out to be different than the parallel case. Up to Re≈152, the vortex shedding is laminar and oblique as exemplified by the smoke-wire photograph in Figure 6 taken at Re≈151, and the corresponding hot-wire spectrum in Figure 7 is dominated by a sharp peak at the shedding frequency.

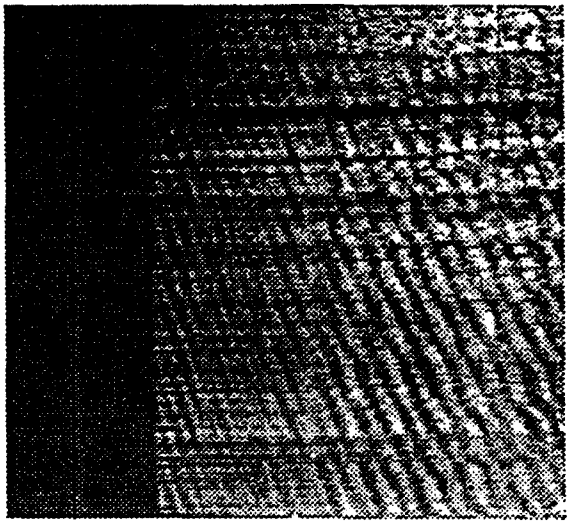

Figure 6. Flow visualization of laminar oblique shedding at Re=151. d=0.157cm, aspect ratio 385. Smoke-wire at x/d=25.

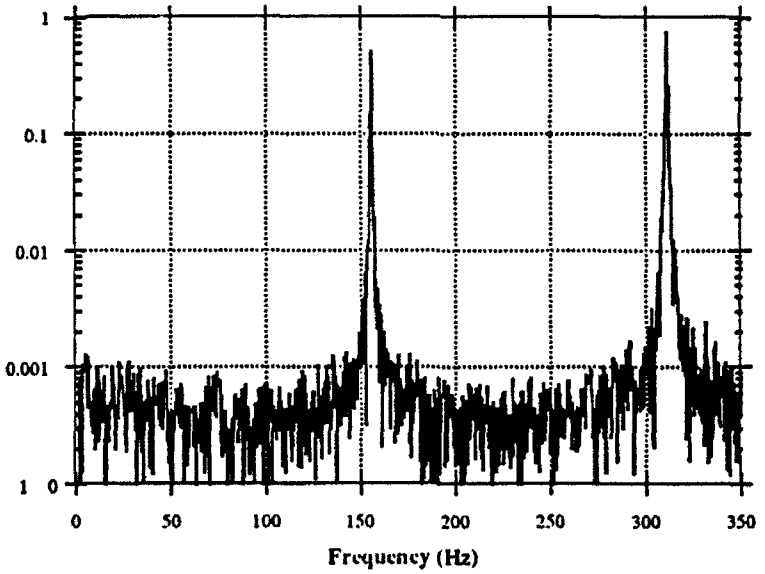

Figure 7. Time-averaged velocity spectrum of laminar oblique shedding at Re=151. d=0.157cm, aspect ratio 385. Hot-wire at x/d=12.

A very small increase of the Reynolds number, in this case to Re≈155, causes the wake to enter a new regime characterized by turbulent spots which appear at random times and spanwise locations, as shown in Figure 8. This causes the hot-wire to register a continually changing frequency spectrum as the shedding frequency becomes unstable. This is illustrated in Figures 9a and 9b which represent two un-averaged velocity spectra at Re=155 taken at different times. The spectrum in Figure 9a is typical of a laminar flow whereas the one in Figure 9b shows a lot of irregularities as a result of the passage of turbulent spots. The corresponding time-averaged spectrum is shown in Figure 9c. This "quasi-turbulent" behavior was observed up to Re≈160, above which the wake is completely turbulent, i.e. the turbulence spreads to the entire span of the cylinder. Figures 10 and 11 represent the flow visualization and frequency spectrum corresponding to this flow. These two last figures closely resemble Figures 2 and 4 respectively.

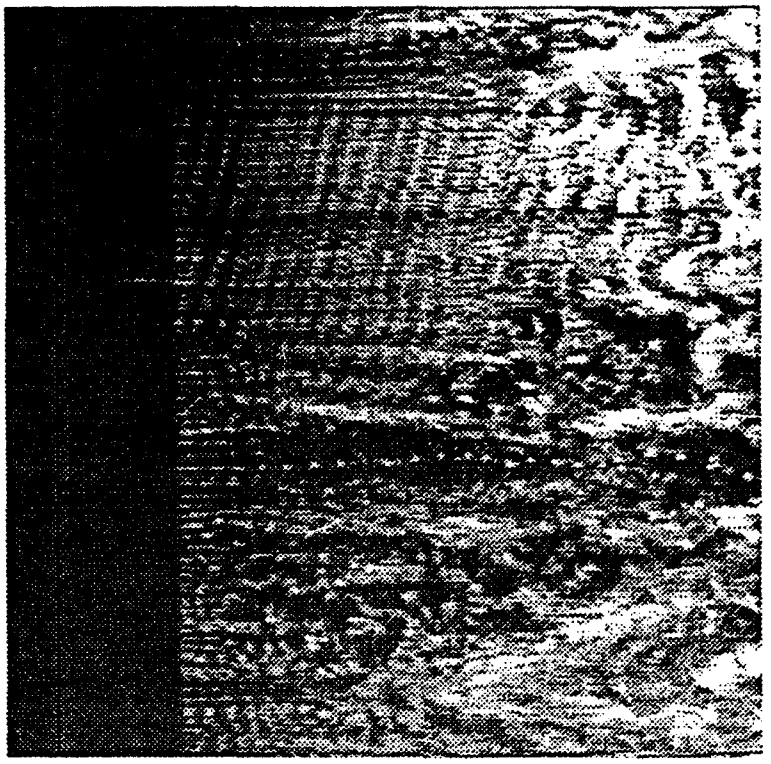

Figure 8. Flow visualization of quasi-turbulent oblique shedding at Re=155. d=0.157cm, aspect ratio 385. Smoke-wire at x/d=25.

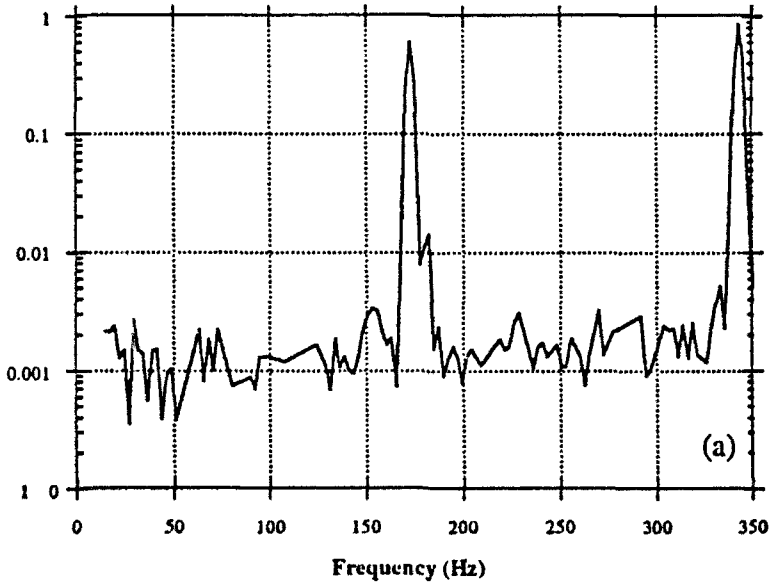

Figure 9a. Non-averaged velocity spectrum of quasi-turbulent oblique shedding at Re=155. d=0.157cm, aspect ratio 385. Hot-wire at x/d=12.

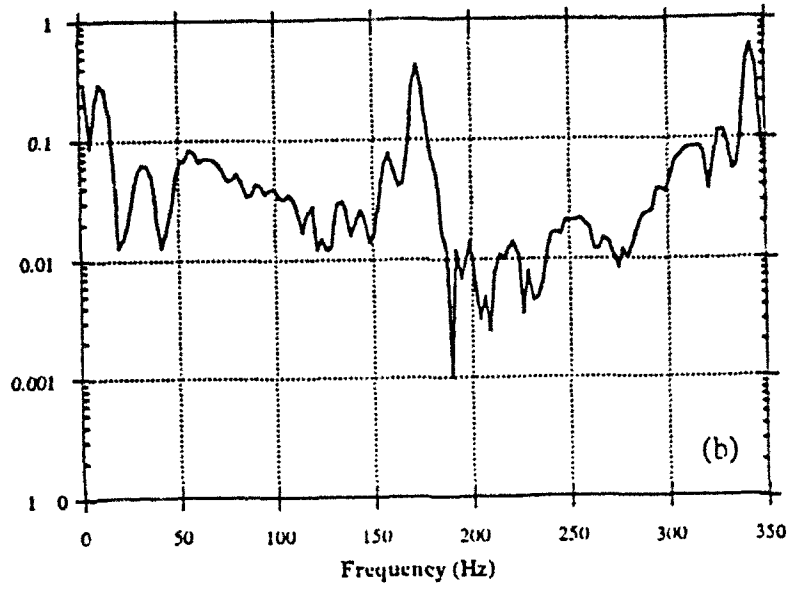

Figure 9b. Non-averaged velocity spectrum of quasi-turbulent oblique shedding at Re=155. d=0.157cm, aspect ratio 385. Hot-wire at x/d=12. Same as in Figure 9a, but at a different instant of

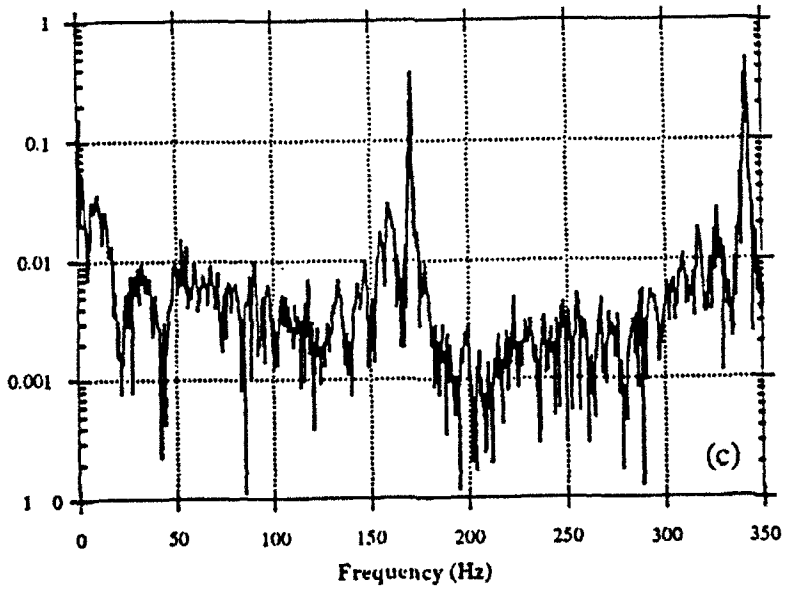

time.

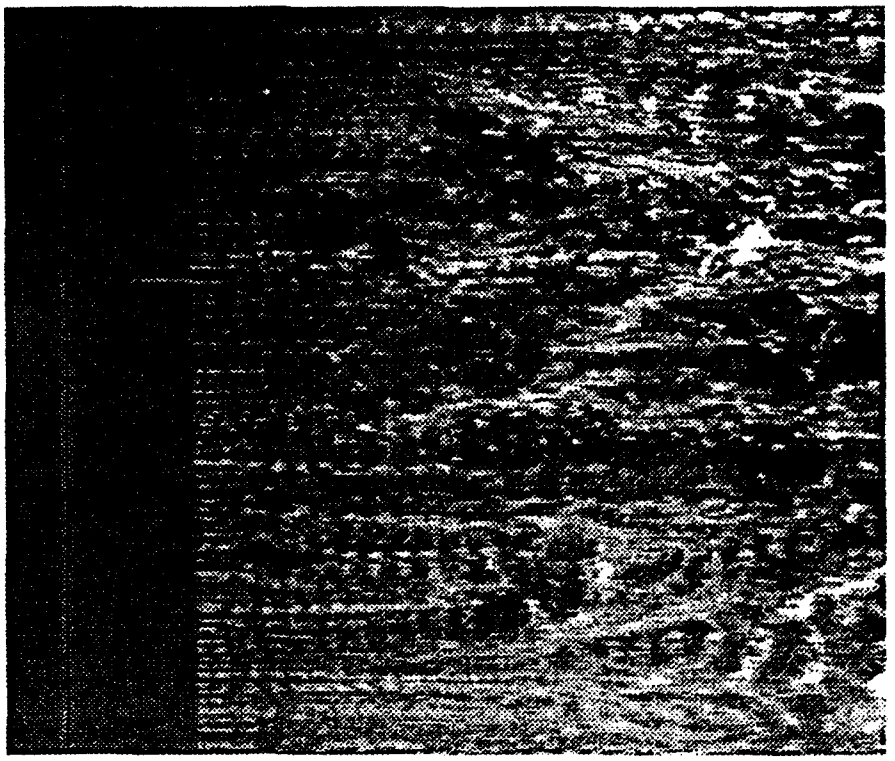

Figure 10. Flow visualization of turbulent shedding at Re=163. d=0.157cm, aspect ratio 385. Smoke-wire at x/d=25.

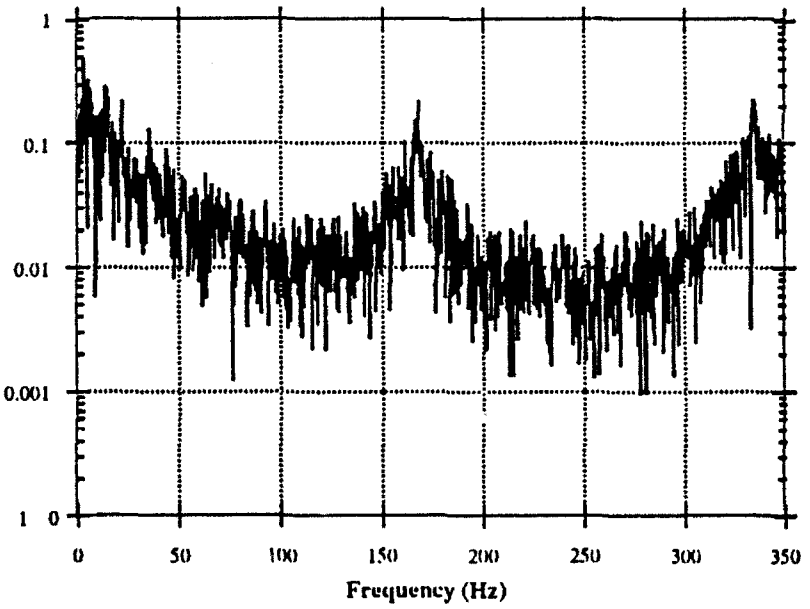

Figure 11. Time-averaged velocity spectrum of turbulent shedding at Re=163. d=0.157cm, aspect ratio 385. Hot-wire at x/d=12.

The root mean square (rms) of velocity fluctuations obtained from the hot-wire measurements described above provide another view of the differences between the parallel and oblique wakes as transition is approached. As shown in Figure 12, the rms of the parallel shedding increases gradually until Re≈164, where it jumps to another regime as the flow suddenly becomes turbulent. The oblique shedding also experiences a gradual increase of the rms level with the Reynolds number but only up to Re≈153, which marks the end of the laminar regime for this case. In the range of Re≈153-163, the rms increases more steeply and has a somewhat erratic trend because the location of the turbulent spots keeps changing. The relatively lower rms values at Re≈155 and Re≈161 for example, can be attributed to the fact that less turbulent spots passed near the location of the hot-wire. Beyond the range Re≈153-163 the rms level is comparable to that of the parallel case as the wake becomes completely turbulent.

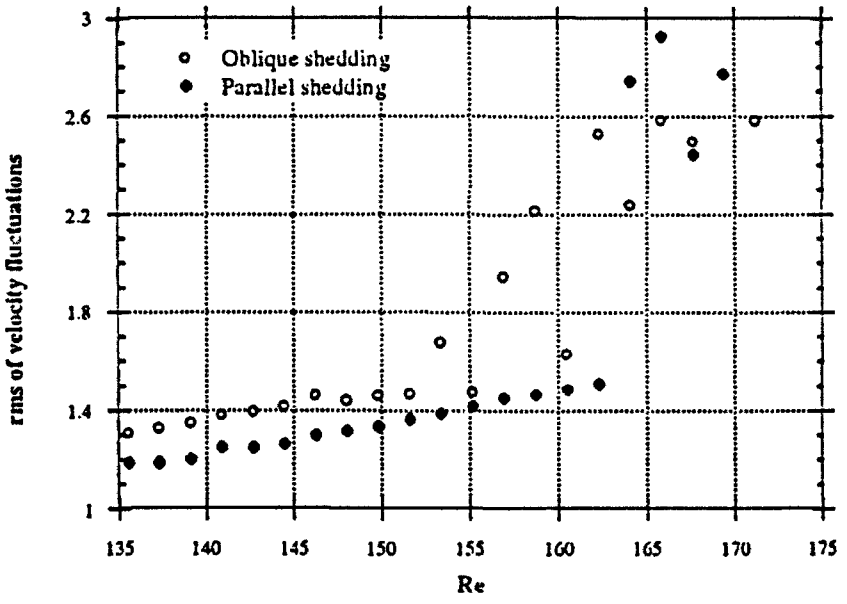

Figure 12. Evolution of root mean square of fluctuating velocity for parallel and oblique shedding with the Reynolds number.

Downstream evolution of the wake:

In these experiments, we focused on the downstream evolution of the parallel and oblique wakes for Reynolds numbers below transition. This was to give an idea of the scales of the three-dimensionality which is present in these wakes prior to their transition to turbulence and help understand why these wakes become turbulent at different Reynolds numbers. Past experimental studies of the wake of circular cylinders for Reynolds numbers below 160 have provided two important, yet seemingly unrelated, observations: The first is that the Kármán vortex street is usually oblique and the second is that three-dimensional structures develop in the far-wake. If we add to these the other important observation that the transition from laminar to turbulent wake occurs at different Reynolds numbers for the parallel and oblique vortex streets, then there is sufficient ground to suspect that the near-wake may contain all the relevant information on the three-dimensionality which is observed in the far-wake of oblique vortex streets and that which is responsible for their transition to turbulence.

Preliminary experiments consisted of smoke-wire flow visualization. Various regions of the wake were visualized with the smoke-wire positioned at a suitable location downstream of the cylinder to avoid any possibility of confusion about the observed structures. The Reynolds number was kept in the range 140-160 for the oblique shedding. In this range of Reynolds numbers, the Kármán vortex street decays by x/d=150 and new vortical structures of larger scale and lower frequency than the primary vortices emerge. This was first observed by Taneda (1959) in towing tank flow visualizations. In their wind tunnel experiments, Cimbala et. al. (1988) demonstrated that the process of reorganization of the wake is controlled by hydrodynamic instability and merely reflects the growth and decay of various frequencies which are present in the system, and not pairing as it had been advanced by Matsui and Okude (1983). Matsui and Okude based their argument in favor of a vortex pairing scenario on flow visualization photographs and measurements of the ratio of the passage frequency of the secondary vortices to the Kármán vortices, f_2/f_1. This ratio happens to be very close to 1/2, even in our experiments but we found that while the shedding frequency f_1 varies with the angle of shedding, the far-wake frequency f_2 remains the same. This further contradicts the idea that the wake reorganizes itself through vortex pairing.

Much like the observations of Cimbala et. al., our smoke-wire flow visualizations showed that the oblique vortices in the near-wake decay and give rise to new vortical structures in the far-wake. Surprisingly, these new vortices start out straight and parallel to the cylinder axis, even though the Kármán vortices were oblique. However, in the case of oblique shedding the secondary structures develop a spanwise waviness further downstream. This waviness amplifies downstream and "breaks" the spanwise rollers into three-dimensional structures equally spaced along the span, in the shape of periodic "lumps". Figures 13a, 13b and 13c, illustrate a sequence of development of an oblique wake with the smoke wire positioned at x/d= 50, 140, and 250 respectively.

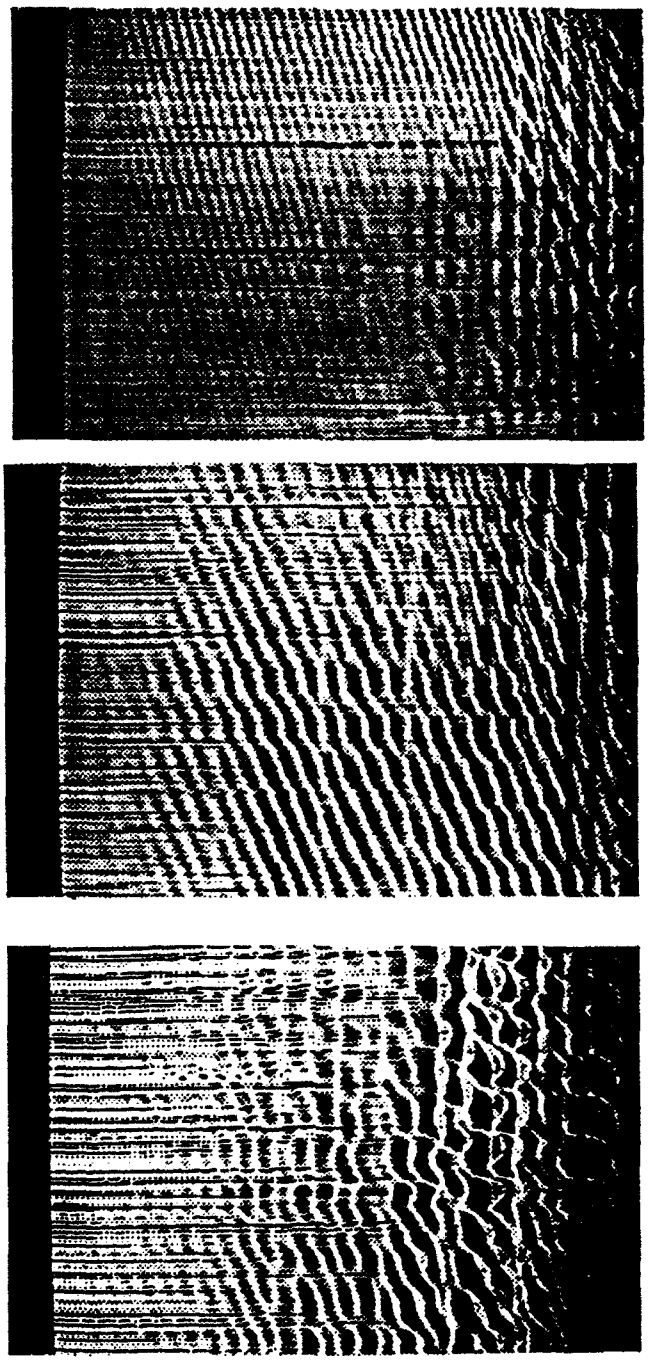

Figures 13a, 13b and 13c. Flow visualization of laminar oblique shedding at Re=140. d=0.106cm, aspect ratio 570. Smoke-wire at x/d=50, 140 and 250 respectively.

The angle of vortex shedding in the near-wake could be changed at any Reynolds number by imposing various flow conditions at the cylinder ends with the control cylinders. As the angle of shedding was varied it became clear that the spanwise size of the "lumps" was affected, suggesting

a link between the near-wake flow condition and the far-wake spanwise "modulation". Making the angle of shedding shallow, i.e. closer to parallel shedding, produced longer "lumps" in the far-wake and making it steeper had the reverse effect. Figures 14a and 14b represent two such cases, where the scale of the three-dimensionality in the far-wake is altered by changing the angle of shedding for the same Reynolds number. The scale in Figure 14a is larger than in Figure 14b.

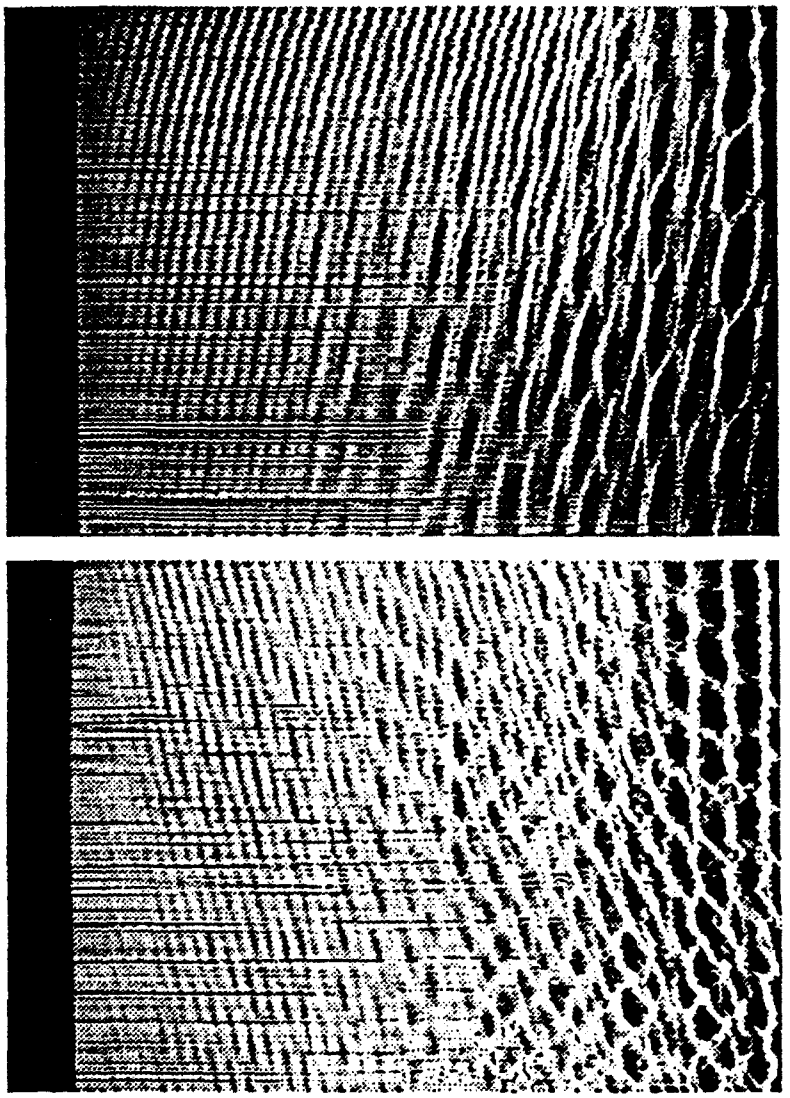

Figure 14a and 14b. The effect of changing the angle of shedding on the scale of the far-wake three-dimensionality. Re=140, d=0.106cm, aspect ratio 570, smoke-wire at x/d=50. in both photographs.

In contrast, the case of parallel shedding produced parallel vortices in the far-wake, such as shown in Figures 15a, 15b and 15c, indicating that the origin of the "lumps" in the far-wake of oblique vortex streets could definitely be traced to some near-wake flow condition.

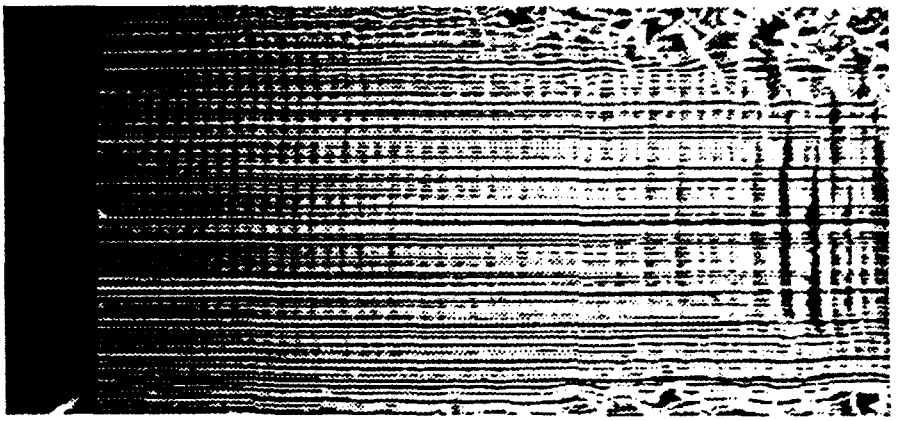

(a)

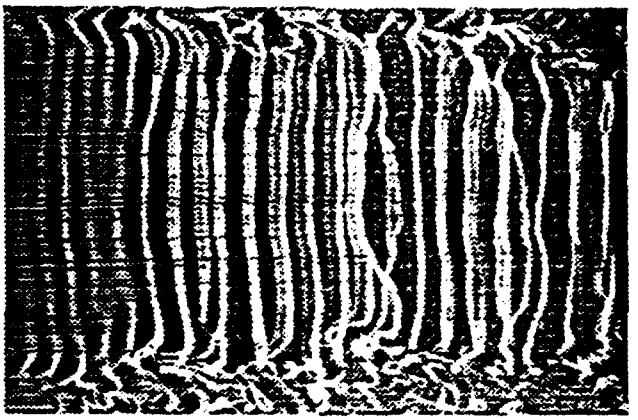

(b)

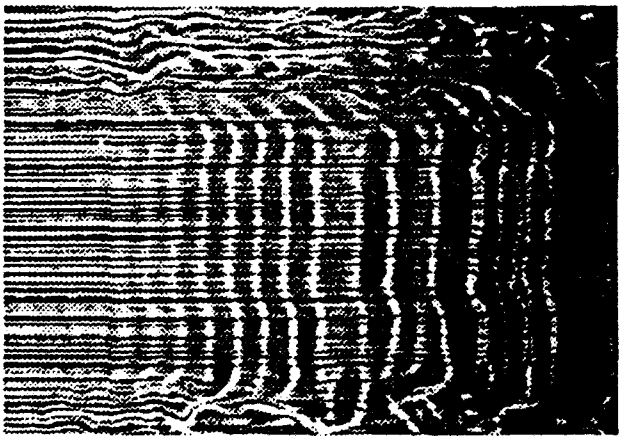

(c)

Figures 15a, 15b and 15c. Flow visualization of laminar parallel shedding at Re=140. d=0.106cm, H/d=220. Smoke-wire at x/d=50, 140 and 250 respectively.

A rather peculiar vortex shedding geometry is depicted in Figure 16 where the vortex shedding goes gradually from parallel (lower portion of the span) to oblique (upper portion). The far-wake also has a different form in the upper and lower portions of the span, which is another indication that the local near-wake shedding condition affects the size of the structures at the corresponding spanwise location in the far-wake.

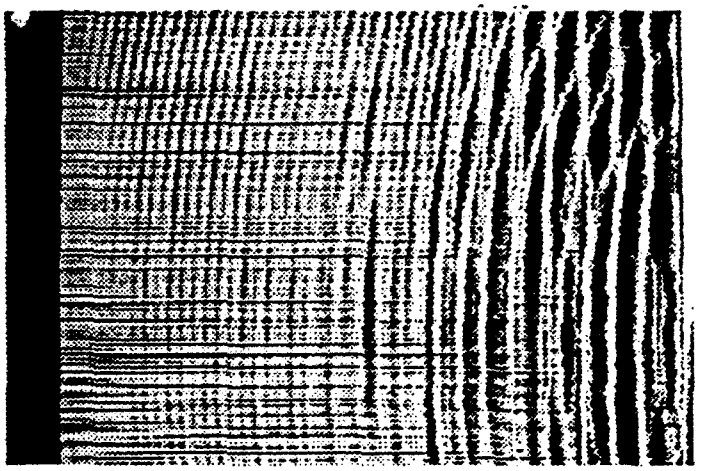

Figure 16. Flow visualization of laminar flow condition in which the shedding angle varies along the span, affecting the scale of the far-wake three-dimensionality. Re=140, d=0.106cm, aspect ratio 570, smoke-wire at x/d=50.

To further investigate the observations described above, time-averaged velocity profiles were taken along the spanwise (z) and cross-stream (y) directions in the wake of the cylinder. The profiles in the cross-stream direction were measured at several spanwise locations in order to look for possible variations in the spanwise direction.

Figures 17a and 17b represent near-wake (x/d=50) profiles in the cross-stream direction at three spanwise stations for the parallel and oblique shedding respectively. As expected, these mean profiles do not show any spanwise variations for either shedding geometry since the mean flow at any spanwise location is identical even for the oblique shedding.

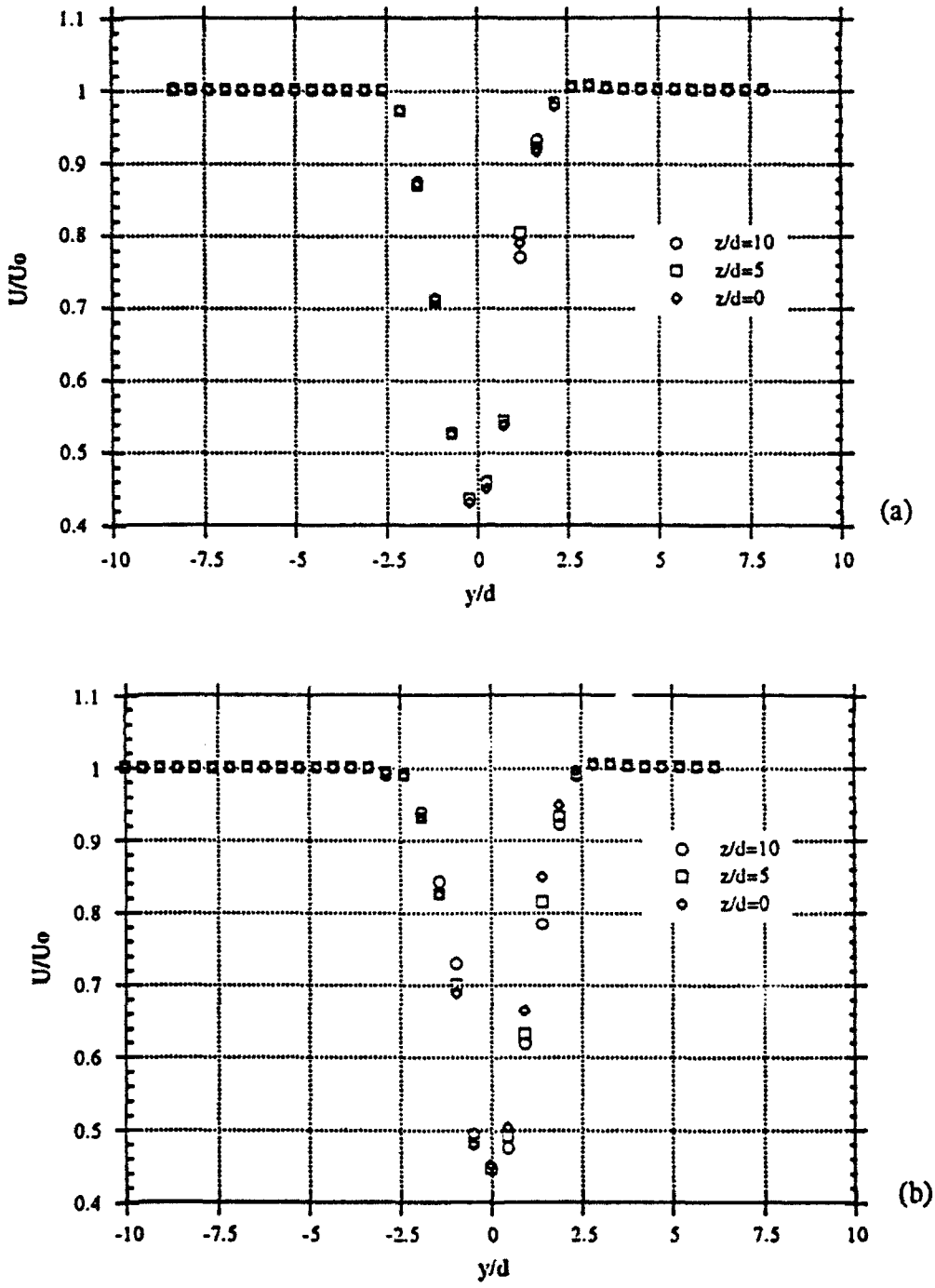

Figure 17a and 17b. Near-wake (x/d=50) velocity profiles in the cross-stream direction at three spanwise stations z/d=0, 5 and 10 at Re=140. (17a) parallel shedding, H/d=220, and (17b) oblique shedding, θ=25°, aspect ratio 570.

The corresponding far-wake data is more interesting, as shown in Figures 18a and 18b for the profiles in the cross-stream direction and Figure 19 for the spanwise direction respectively. Six such profiles were measured at regular spanwise locations for the two shedding geometries. All six profiles in the cross-flow direction are identical for the parallel shedding, but they present a good deal of scatter for the oblique shedding. The spanwise velocity profile is relatively flat for the parallel shedding case whereas it is periodic for the oblique case. We noted that the wavelength of the spanwise velocity profile closely matches the "wavelength" of the lumps observed by flow visualization. It was also established that the minima coincide with the region of maximum thickness of the lumps while the maxima in the spanwise velocity profile coincide with the regions between the lumps (see Figure 23). Once the far-wake vortices adopt the shape shown at the right edge of Figure 13c, their local diameter varies with the spanwise direction in a periodic pattern and their induced velocity varies inversely with the local diameter.

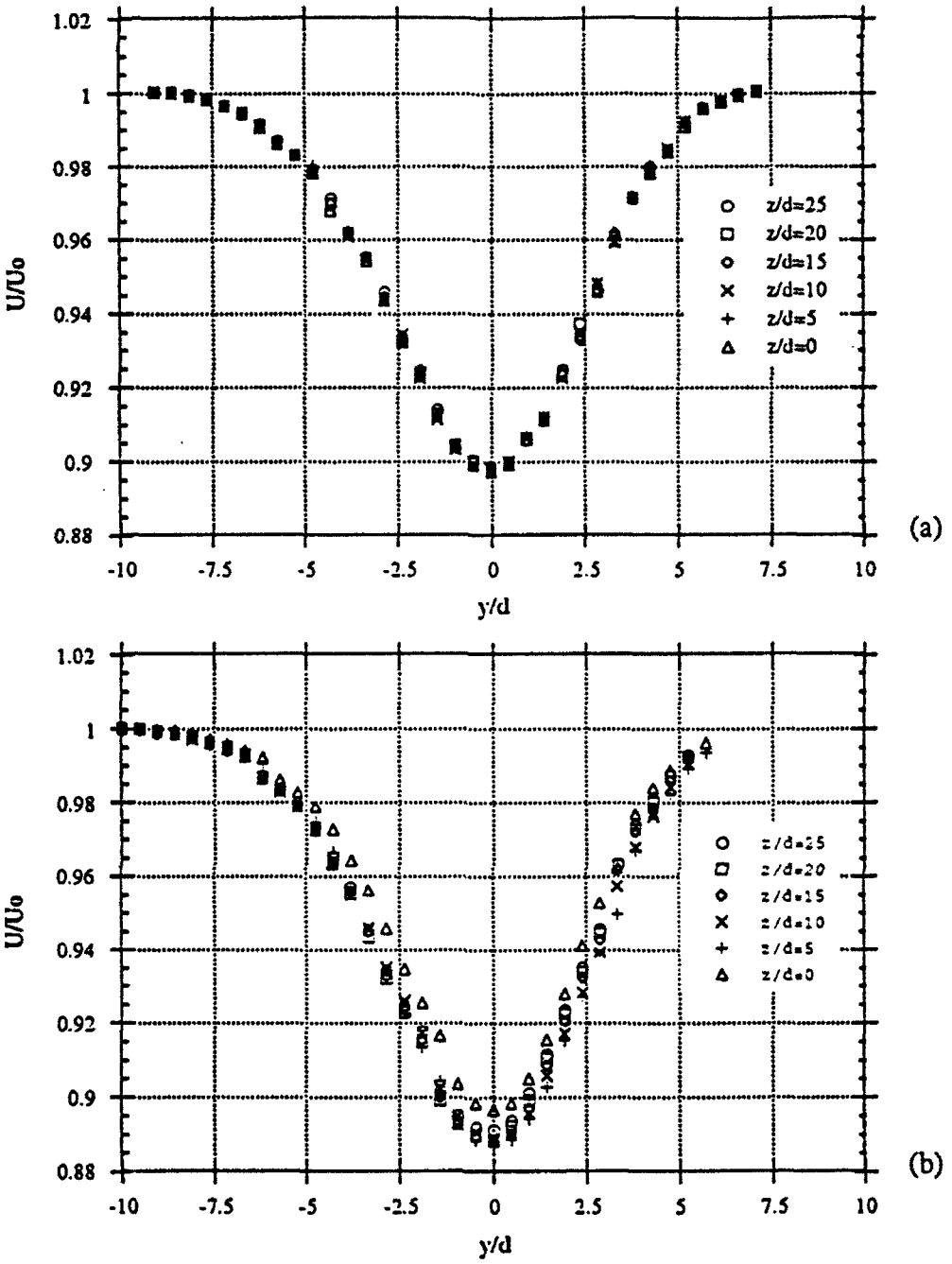

Figures 18a and 18b. Far-wake (x/d=360) velocity profiles in the cross-stream direction at six spanwise stations z/d=0, 5, 10, 15, 20 and 25 at Re= 140. (18a) parallel shedding, H/d=220, and (18b) oblique shedding, θ=25°, aspect ratio 570.

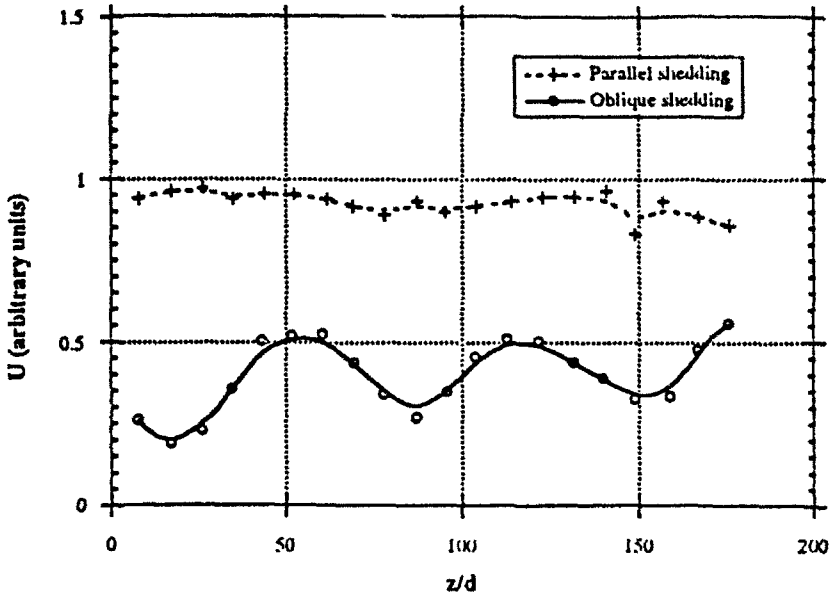

Figure 19. Far-wake (x/d=360) profiles in the spanwise direction at the center of the wake for the parallel and oblique shedding corresponding to Figures 18a and 18b.

Time-averaged velocity profiles in the spanwise direction were taken at various downstream locations. Two of these profiles are represented in Figure 20 which shows that the structures observed in the far-wake of oblique vortex streets are phase-locked in space *in the mean*. This phase-locking of the vortices is thought to be reached as a result of the induction of each vortex on the next one.

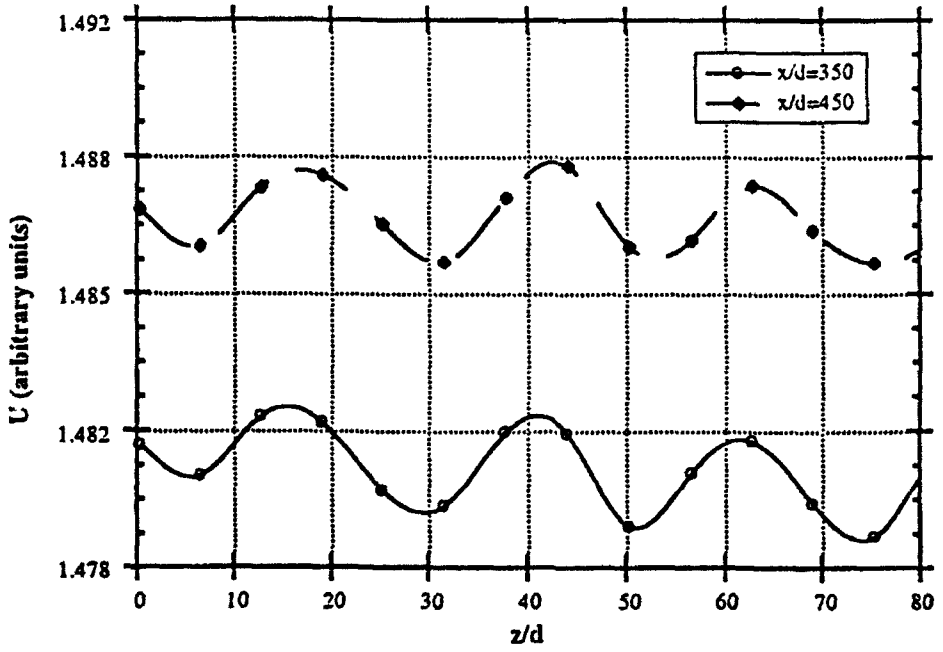

Figure 20. Velocity profiles in the spanwise direction for oblique shedding measured at x/d= 350 and 450, y=0. Re=140, θ=22°, aspect ratio 570.

As was mentioned earlier, flow visualization unveiled a direct dependence of the scale of the far-wake three-dimensionality on the near-wake angle of shedding. It is clear that the mean velocity profiles in the near-wake do not outline any sort of three-dimensionality. The alternative was then to measure the spanwise wavelength of vortex shedding, i.e. the spacing between two consecutive Kármán vortices of the same sign. This wavelength was determined by measuring the phase shift between the signals measured by two hot-wires which could be moved with respect to each other in the spanwise direction. It turns out that this wavelength is equal to the wavelength of the corresponding spanwise mean velocity profile in the far-wake, and therefore also equal to the spanwise scale of the "lumps" in the far-wake. Figure 21 represents the variation of the phase shift with the spacing between the hot-wire probes in the near-wake and Figure 22 the corresponding mean spanwise velocity profile in the far-wake. From these two figures it is easy to determine that the spanwise wavelengths in the near- and far-wakes are equal.

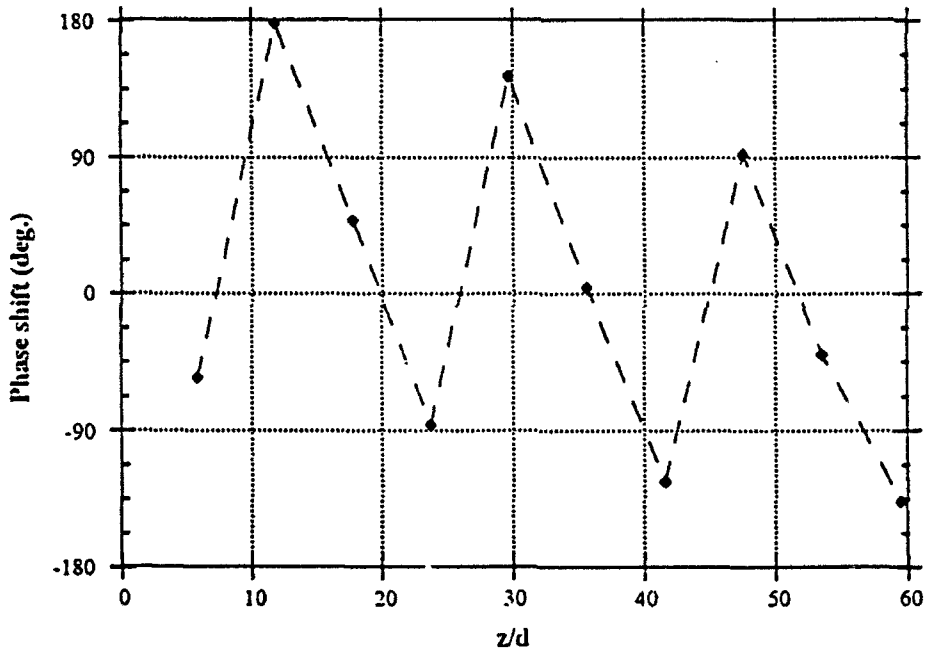

Figure 21. Variation of the phase shift with the spacing between the hot-wire probes in the near-wake of oblique shedding.

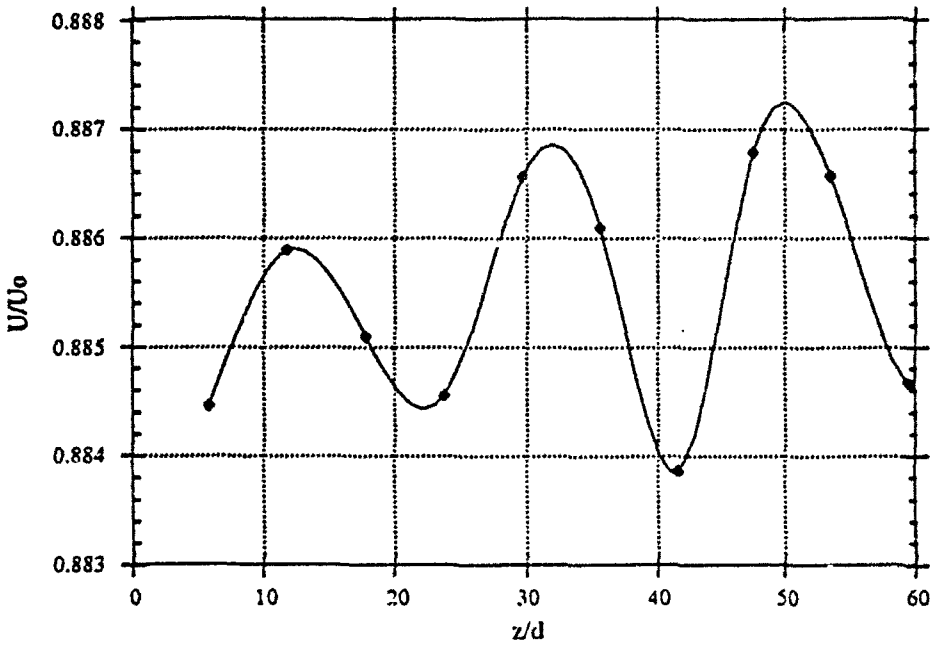

Figure 22. Mean velocity profile in the spanwise direction in the far-wake of the flow corresponding to Figure 21.

Figure 23 is a schematic representing the near- and far-wake spanwise wavelengths as well as the locations of higher and lower mean velocity in the far-wake.

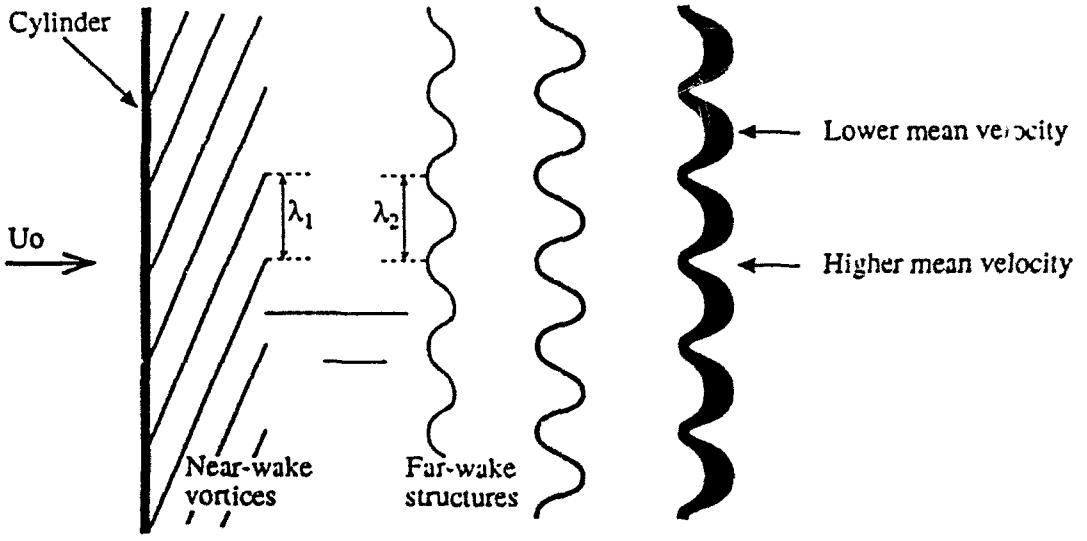

Figure 23. Schematic of wavelength in the near- and far-wake and location of higher and lower mean velocity in the far-wake for oblique shedding.

After we used two hot-wires to measure the spanwise wavelength in the near-wake and showed that it is equal to the wavelength in the far-wake for a few typical cases, we found a good correspondence between the smoke-wire flow visualization photographs and the hot-wire measurements and that the photographs could be digitized and the spanwise wavelength measured from them with good accuracy. We then reverted to this method to investigate various combinations of Reynolds numbers, angles of shedding and cylinder diameters. Each flow condition was represented by a pair of photos: one for the near-wake and another one for the far-wake. These photos were then digitized and the near-wake and far-wake spanwise wavelengths, denoted by $\lambda 1$ and $\lambda 2$ respectively, were measured directly from the computer images. The results, shown in Figure 24, confirm that the near- and far-wake wavelengths are equal for oblique shedding for all the cases we observed.

As was reported in Hammache and Gharib (1990), the oblique shedding is due to a base pressure imbalance between the cylinder ends. This in turn induces a spanwise flow in the base region of the cylinder which excites an oblique "mode" of vortex shedding. Once the vortices shed obliquely, at a frequency f_1, the vorticity vector is comprised of a component in the spanwise direction and one in the streamwise direction, ω_z and ω_x respectively. This vortex street eventually dies out, the mean velocity profile becomes unstable and a new vortex pattern emerges with a frequency f_2. It is likely that the streamwise component ω_z does not decay, but rather interacts with the spanwise component in the far-wake to produce the spanwise modulation of the secondary vortices which become increasingly three-dimensional with the downstream distance. As the Reynolds number is gradually increased to approximately 152, the wake reaches the transition from laminar to turbulent flow. This transition is favored by the relatively large-scale three-dimensionality described above. In contrast, the parallel shedding case remains laminar until the Reynolds number is above 165 (and even higher for lower cylinder length/diameter aspect ratios.) As the parallel wake transition is approached, the secondary vortices develop an instability which manifests itself in the shape of "wiggles" of small scale than the lumps which characterize the oblique case. These wiggles appear randomly on the vortices and do not have a specific wavelength. As the Reynolds number is increased (but still kept below transition), the mean spanwise velocity profile of the parallel wake case develops random bumps which are considerably smaller than the periodic variations of the oblique case and remains relatively flat in comparison.

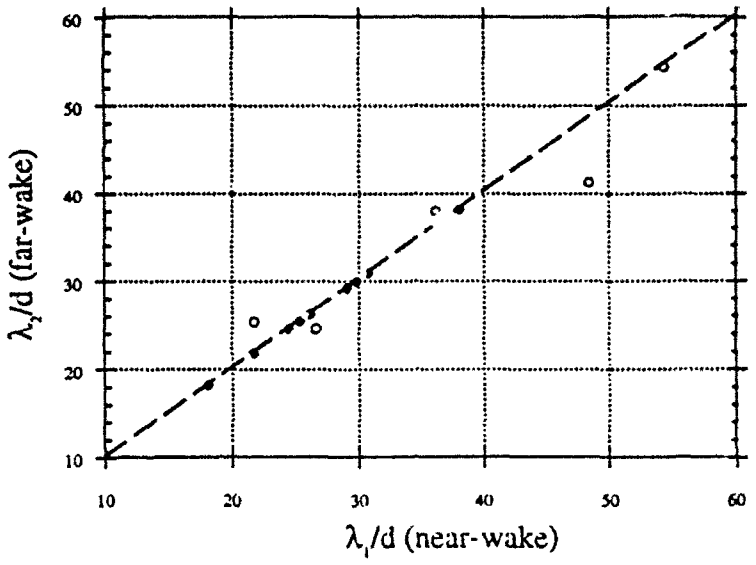

Figure 24. Plot of near-wake versus far-wake wavelengths for various Reynolds numbers, cylinder diameters and angles of shedding.

Conclusion:

We can conclude that the parallel and oblique wakes undergo distinct transitions to turbulence: the parallel case experiences a sharp transition from laminar to turbulent wake, while the oblique case goes from laminar to turbulent via a regime in which the wake is partly laminar and partly turbulent. The turbulence in this regime appears as random spots along the cylinder span. It is possible that when the Reynolds number is in the "quasi-turbulent" regime, the angle of vortex shedding is no longer stable and the wake can consist of vortices which bend at one or several points along the span. The two regions on either side of the "bend" do not necessarily have the same angle and thus the same frequency. A frequency mismatch at the interface creates turbulent spots similar to those observed behind the nodes of vibrating cylinders by Van Atta, Gharib and Hammache (1988) and behind a region of local discontinuity in the cylinder diameter by Lewis and Gharib (1992). Oblique vortex streets already have a three-dimensionality at Reynolds numbers below transition which favors an early transition, whereas parallel vortex streets remain laminar longer and their transition happens when the vortices themselves develop three-dimensional features.

As far as the downstream evolution of the oblique wake is concerned, we conjecture that once the Kármán vortex street decays, the spanwise wavelength (spanwise distance between two consecutive vortices of the same sign of vorticity) survives and modulates the secondary structure of the far-wake. In this respect, the three-dimensionality which marks the far-wake vortices is a result of the interaction of the spanwise wavelength in the near-wake and the streamwise wavelength of the far-wake. This is in agreement with the results of experiments conducted by Corke et. al. (1992) on the interaction of plane Tollmien-Schlichting waves and pairs of oblique waves in the wake of an airfoil.

Acknowledgements:

We kindly thank Professor P.J. Strykowsky for pointing out an error which slipped in both Hammache and Gharib papers (1989 and 1991), in which the following equation was suggested for the Strouhal vs Reynolds number relationship to fit the data for parallel shedding:

$St_0 = 0.212 - 5.35/Re$

This equation should be replaced by:
$St_0 = 0.1871 - 3.6264/Re + 15x10^{-5}Re.$

This work was supported by a grant from the Office of Naval Research, Division of Ocean Engineering, contract No. N0014-90-J-1314

List of Figures:

Figures 13a, 13b and 13c. Flow visualization of laminar oblique shedding at Re=140. d=0.106cm, aspect ratio 570. Smoke-wire at x/d=50, 140 and 250 respectively.

Figure 14a and 14b. The effect of changing the angle of shedding on the scale of the far-wake three-dimensionality. Re=140, d=0.106cm, aspect ratio 570, smoke-wire at x/d=50.

Figures 15a, 15b and 15c. Flow visualization of laminar parallel shedding at Re=140. d=0.106cm, H/d=220. Smoke-wire at x/d=50, 140 and 250 respectively.

Figure 16. Flow visualization of laminar flow condition in which the shedding angle varies along the span, affecting the scale of the far-wake three-dimensionality. Re=140, d=0.106cm, aspect ratio 570, smoke-wire at x/d=50.

Figure 17a and 17b. Near-wake (x/d=50) velocity profiles in the cross-stream direction at three spanwise stations z/d=0, 5 and 10 at Re=140. (17a) parallel shedding, H/d=220, and (17b) oblique shedding, θ=25°, aspect ratio 570.

Figures 18a and 18b. Far-wake (x/d=360) velocity profiles in the cross-stream direction at six spanwise stations z/d=0, 5, 10, 15, 20 and 25 at Re= 140. (18a) parallel shedding, H/d=220, and (18b) oblique shedding, θ=25°, aspect ratio 570.

Figure 19. Far-wake (x/d=360) profiles in the spanwise direction at the center of the wake for the parallel and oblique shedding corresponding to Figures 18a and 18b.

Figure 20. Velocity profiles in the spanwise direction for oblique shedding measured at x/d= 350 and 450, y=0. Re=140, θ=22°, aspect ratio 750.

Figure 22. Mean velocity profile in the spanwise direction in the far-wake of the flow corresponding to Figure 21

Figure 22. Mean spanwise velocity profile in the far-wake of the flow corresponding to Figure 21.

Figure 23. Schematic of wavelength in the near- and far-wake and location of higher and lower mean velocity in the far-wake for oblique shedding.

Figure 24. Plot of near-wake versus far-wake wavelengths for various Reynolds numbers, cylinder diameters and angles of shedding.

References:

Cimbala, J.M., Nagib, H.M. & Roshko, A. (1988). Large structure in the far-wakes of two-dimensional bluff bodies. *J. Fluid Mech.* 190, 265-298.

Corke, T.C., Krull, J.D. & Ghassemi, M. (1992). Three-dimensional-mode resonance in far-wakes. *J. Fluid Mech.* 239, 99-132.

Eisenlohr, H. & Eckelmann, H. (1989). Vortex splitting and its consequences in the vortex street wake of cylinders at low Reynolds number. *Phys. Fluids* A1, 189-192.

Hammache, M. & Gharib, M. (1989). A novel method to promote parallel vortex shedding in the wake of circular cylinders. *Phys. Fluids* A1, 1611-1614.

Hammache, M. & Gharib, M. (1991). An experimental study of the parallel and oblique vortex shedding from circular cylinders. *J. Fluid Mech.* 232, 567-590.

Lewis, C.G. & Gharib, M. (1992). An exploration of the wake three-dimensionalities caused by a local discontinuity in cylinder diameter. *Phys. Fluids* A1, 104-117.

Matsui,T. & Okude, M. (1983). Formation of the secondary vortex street in the wake of a circular cylinder. In *Structure of Complex Turbulent Shear Flow, IUTAM Symposium, Marseille*. Springer.

Taneda, S. (1959). Downstream development of the wakes behind cylinders. *J. Phys. Soc. Japan*, vol. 14, No. 6, 843-848.

Van Atta, C., Gharib, M. & Hammache, M. (1988). Three-dimensional structure of ordered and chaotic vortex streets behind circular cylinders at low Reynolds numbers. *Fluid Dyn. Res.* vol 3, 127-132

Williamson, C.H.K. (1988). Defining a universal and continuous Strouhal-Reynolds number relationship for the laminar vortex shedding of a circular cylinder. *Phys. Fluids* 31, 2742-2744.

Williamson, C.H.K. (1992). Three-dimensional phenomena in bluff body wakes. *Abstract, IUTAM Symposium on Bluff body wakes, dynamics and instabilities, Göttingen.*